

ELECTRONIC SUPPLEMENTARY INFORMATION

Cyclic peptide scaffold with ability to stabilize and deliver a helical cell-impermeable cargo across membranes of cultured cancer cells

Nicole Lawrence,^{1‡*} Grégoire J.-B. Philippe,^{1‡} Peta J. Harvey,¹ Nicholas D. Condon,¹ Aurélie H. Benfield,^{1,2} Olivier Cheneval,¹ David J. Craik,^{1*} Sónia Troeira Henriques^{1,2*}

‡ These authors contributed equally.

¹ Institute for Molecular Bioscience, The University of Queensland, Brisbane, Queensland 4072, Australia

² Queensland University of Technology, School of Biomedical Sciences, Institute of Health & Biomedical Innovation and Translational Research Institute, Brisbane, Queensland, 4102, Australia

Corresponding Authors

* Tel. +61 7 33462014 E-mail: n.lawrence@imb.uq.edu.au

* Tel. +61 7 33462019 E-mail: d.craik@imb.uq.edu.au

* Tel. +61 7 34437342 E-mail: sonia.henriques@qut.edu.au

Table S1. Comparison of peptide binding and lysis of model membranes composed of POPC and POPC/POPS (4:1)

Peptide	POPC			POPC/POPS (4:1)			Lytic selectivity (PS/PC) ^d
	P/L 16 μ M ^a (mol/mol)	P/L _{max} ^b (mol/mol)	Leakage LC ₅₀ (μ M) ^c	P/L 16 μ M (mol/mol)	P/L _{max} ^b (mol/mol)	Leakage LC ₅₀ (μ M) ^c	
PF4PD	0.05	0.11 \pm 0.11	2.7 \pm 0.4	0.12	0.29 \pm 0.17	0.02 \pm 0.002	135
cPF4PD	0.03	0.03 \pm 0.01	9.9 \pm 2.3	0.08	~ 0.4	0.06 \pm 0.01	165
ctPF4PD	0.04	0.04 \pm 0.01	5.4 \pm 1.3	0.09	0.11 \pm 0.01	0.22 \pm 0.01	24.5
PF4P_pDI	0.09 ^e	-	0.4 \pm 0.02	0.18 ^e	-	0.16 \pm 0.01	2.5
cPF4Pext_pDI	0.05	0.11 \pm 0.04	8.5 \pm 1.2	0.14	^f	0.32 \pm 0.02	26.5
ctPF4P_pDI	0.04	0.05 \pm 0.01	>>10	0.02	0.10 \pm 0.19	4.7 \pm 0.2	-
Melittin			0.3 \pm 0.01			0.15 \pm 0.01	2

^a Peptide to lipid ratio (P/L, mol/mol) at the end of the association phase for 16 μ M peptide (t=170s).

^b P/L_{max} refers to the P/L obtained when peptide-lipid binding reaches saturation and was determined from fitting the dose response curves (see Figure 3A). Error values are associated with the curve fit from single dose experiments.

^c Peptide concentration required to induce leakage of 50% of the vesicles (LC₅₀) was determined from the dose response curves (see Figure 3B). Error values are SD from three technical replicates from a single experiment.

^d Lytic selectivity for POPC/POPS (4:1) membranes was determined relative to POPC for each of the peptides.

^e P/L was determined from the maximum binding achieved prior to lipid loss from the L1 chip (t~10s).

^f Binding did not reach a plateau, therefore P/L_{max} could not be accurately determined.

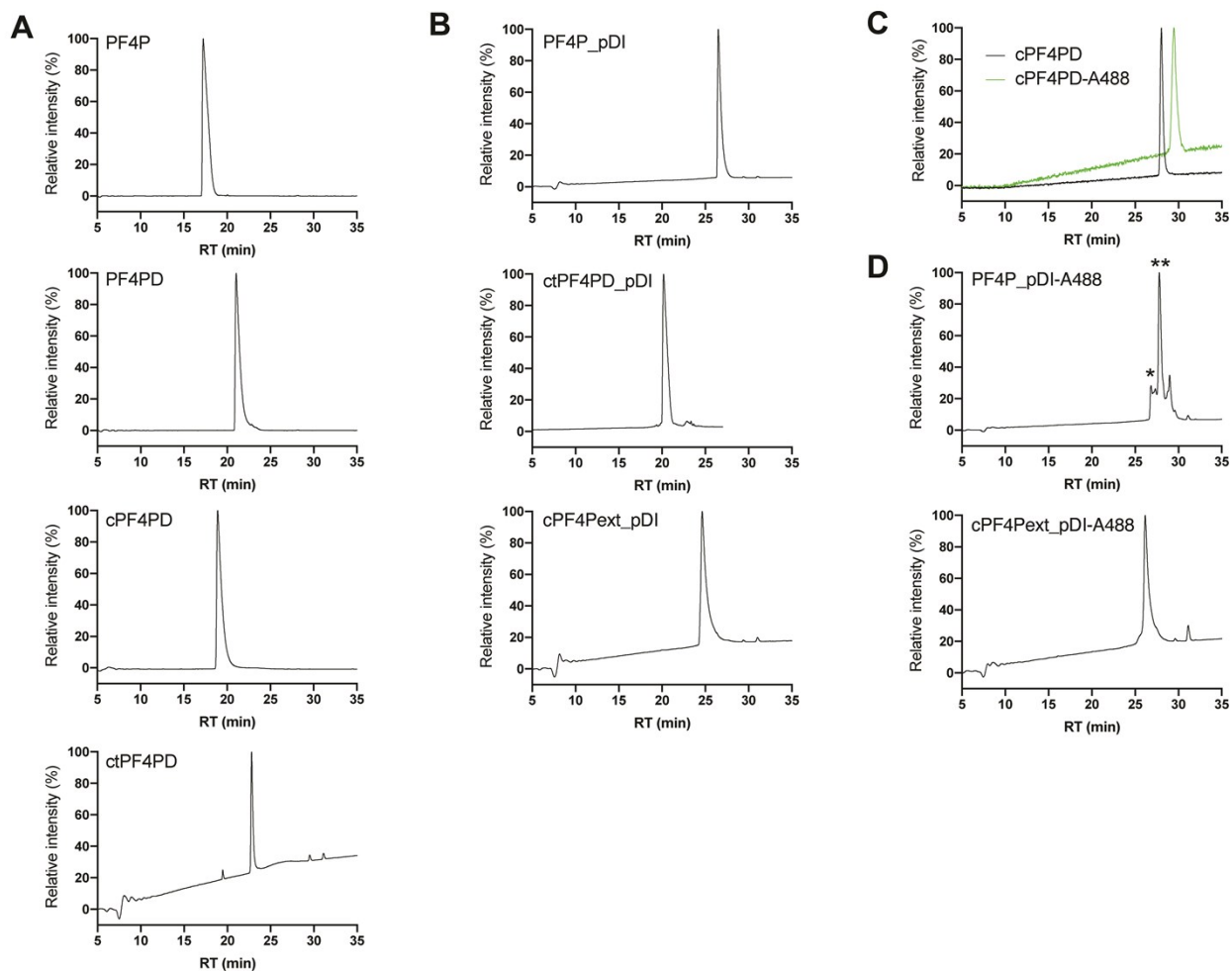


Figure S1. Analytical HPLC trace for peptides showing purity. Peptides (~ 0.1 mg) were dissolved in 50 μ l of 0.1% formic acid (v/v in water) and run on analytical RP-HPLC with a 2% min^{-1} gradient of 90% acetonitrile, 0.1% formic acid (v/v), starting from 1% acetonitrile, 0.1% formic acid (A, B, D); or a 2% min^{-1} gradient of 90% acetonitrile, 0.05% TFA (v/v), starting from 1% acetonitrile, 0.1% TFA (C) . Retention time (RT) is shown, but is not directly compared between peptides, as these data have been compiled from different runs, solvents and instruments. (A) PF4P scaffold peptides; (B) PF4P grafted peptides; (C) cPF4PD and cPF4PD labeled with Alexa Fluor 488 (cPF4PD-A488) have a very similar retention time, suggesting minimal change in hydrophobicity. We have previously demonstrated that cPF4PD and cPF4PD-A488 have near-identical membrane binding properties;¹ (D) pDI grafted peptides with A88 label. For PF4P_pDI, the main peak corresponds to PF4P_pDI with a single A88 label (**), a peak with a shorter RT corresponds to unlabeled peptide (*), and a peak with a longer RT may correspond to an additional, non-covalently attached A88 label, or a cis/trans isomer. (Note, it was difficult to purify unlabeled from labeled PF4P_pDI due to the RTs being very close together. PF4P_pDI had the longest RT of any of the peptides included in this study, see **Table 1**). The A88 dye is located on an inter-helix loop for PF4P_pDI and cPF4Pext_pDI (similar to cPF4PD), so we do not expect the label to affect how these peptides interact with membranes either.

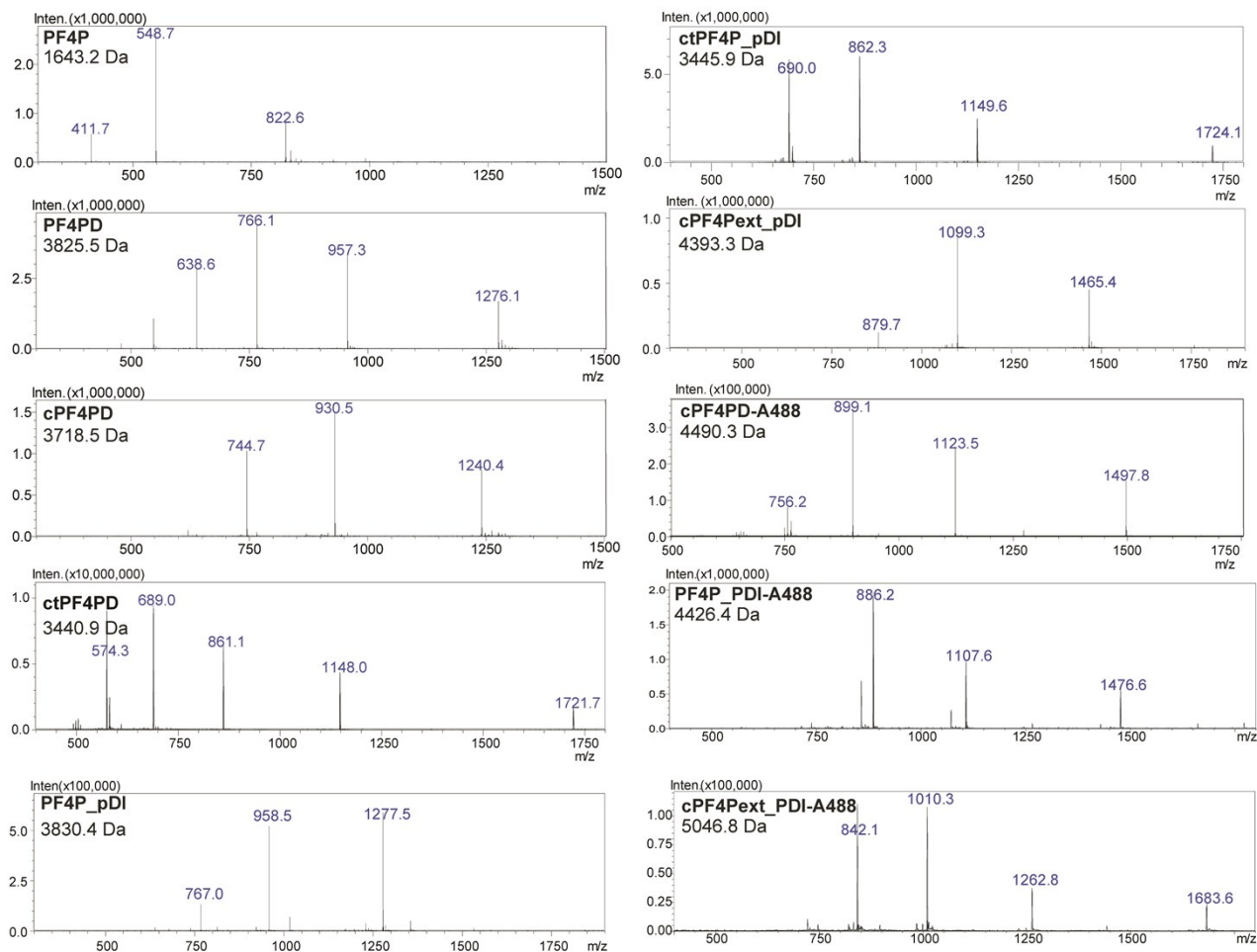


Figure S2. Mass determination of peptides. MS trace with m/z peaks indicating peptide size and purity. Correct peptide mass was determined by dissolving ~ 0.1 mg peptide in 0.1% TFA and directly injecting onto ESI-MS. Peptide mass was determined using the formula: $\text{mass} = (\text{m/z} \cdot z) - z$, where z is the charge of the ion.

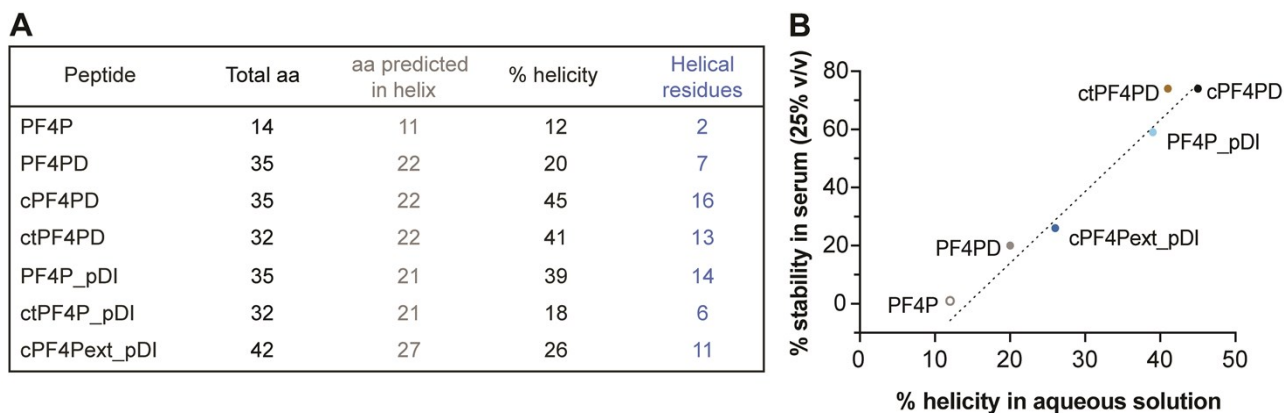


Figure S3. Comparison of the overall helicity of peptides and resistance to degradation in human serum. (A) Helicity was determined from CD spectra of 50 μM peptides in aqueous solution (100 mM NaF, 10 mM KH_2PO_4 [pH 7.5]). Predicted aa in helix (grey) was determined from the relative number of residues expected to contribute to an α -helix, based on the structure of PF4 (PDB:1F9Q) and pDI primary sequence; % helicity was calculated from CD spectra of 50 μM peptide in water using the formula, $H_\alpha = (\theta_{222\text{nm}} - \theta_C) / (\theta_{222\text{nm}}^\infty - \theta_C)$, where $\theta_{222\text{nm}}$ is the lowest value between 218 and 222nm, $\theta_C = 2220 - 53T$ and $\theta_{222\text{nm}}^\infty = (-44000 + 250T)(1 - k / N_{\text{res}})$ with T in $^\circ\text{C}$ and $k=3.0$. [$\theta = m\text{deg} / (c \cdot l \cdot N_{\text{res}})$, where $m\text{deg}$ is the CD output in millidegrees, c is the molar peptide concentration, l is the light path length in mm and N_{res} is the number of amino acid residues]; actual helical residues (blue) calculated as % helicity x total aa. (B) Positive correlation between the % helicity and % stability in human serum for peptide scaffolds and grafts.

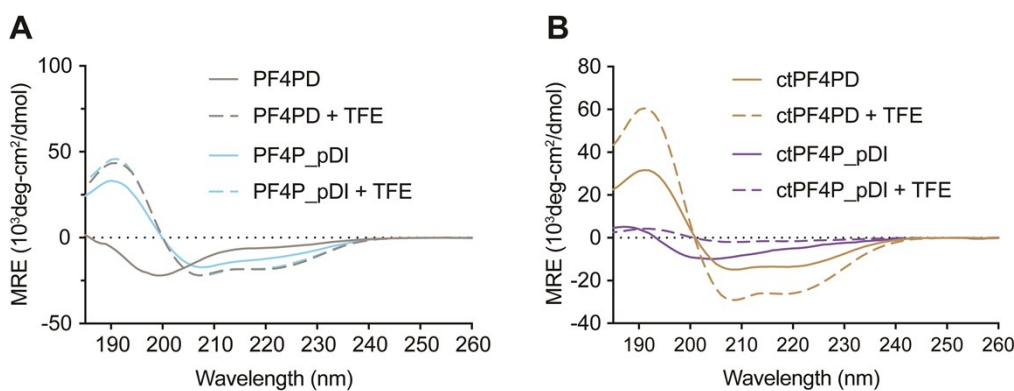


Figure S4. CD spectra of peptides in aqueous and hydrophobic solutions. (A) Open format peptides. (B) Cyclic peptides (thioether, ct). The presence of α -helical structure is indicated by mean residual ellipticity (MRE) minima at 208 and 222 nm. Spectra for peptides in aqueous solution are shown with solid lines, and with 50% trifluoroethanol (TFE) with dashed lines. Peptides that become helical in the less polar TFE solution have propensity to acquire α -helical structure in the presence of membranes. It is not possible to directly measure the spectra of these peptides in the presence of lipid vesicles, as the peptides are highly membrane disruptive and induce lipid precipitation at concentrations required to obtain good CD signal (e.g. using 50 μM peptide and 500 μM of lipid to achieve a peptide-to-lipid ratio of 1:10 and a good signal-to-noise).

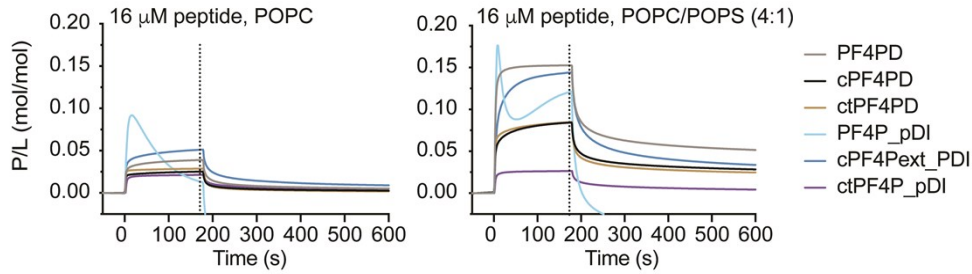


Figure S5. Binding of PF4 scaffold and grafted peptides to model membranes. Peptides were injected over lipid bilayers composed of POPC or POPC/POPC (4:1 mol/mol) deposited on the surface of an L1 chip. The surface plasmon resonance (SPR) response units (RU) were converted to peptide to lipid ratio (P/L, mol/mol) by assuming 1 RU = 1 pg mm⁻². Representative SPR sensorgrams showing peptide P/L obtained with 16 μM peptide are shown here. P/L values that were recorded at the end of the association phase (t=170s, dotted line) are shown in dose-response curves in **Figure 3**.

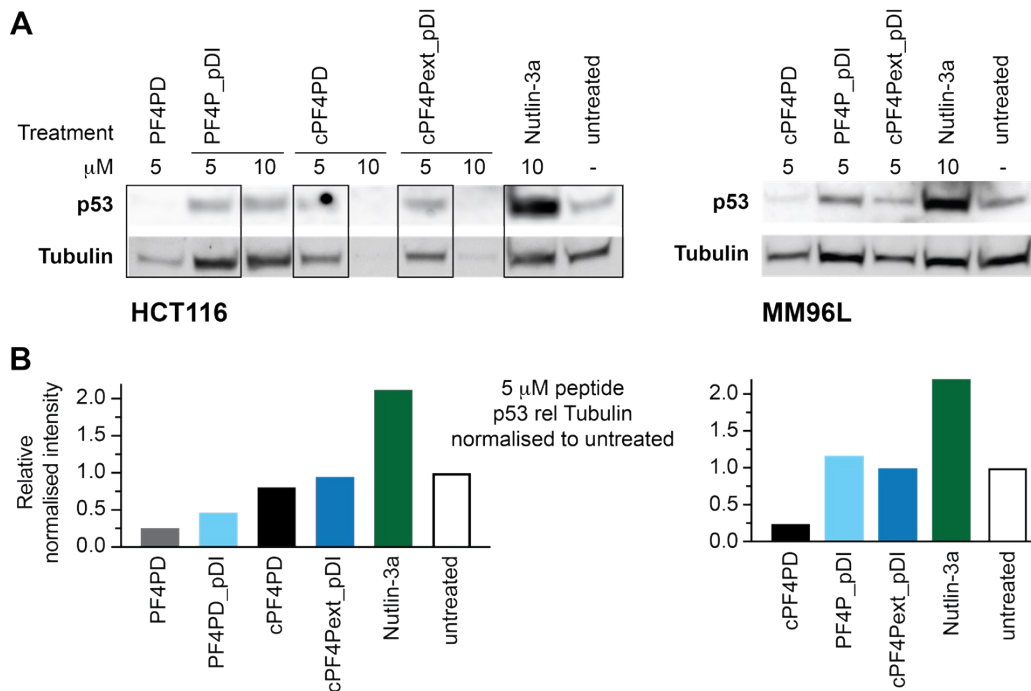


Figure S6: Expression of p53 in HCT116 and MM96L cells following treatment with peptides. (A) Western blot showing expression of p53 and Tubulin. Protein extracts were obtained from cells after 24 h treatment. Nutlin-3a was included as a positive control for p53 reactivation. (B) Relative intensity of p53 relative to Tubulin from western blots. Values were normalized according to the intensity recorded for untreated cells. Densitometry measurements were determined for area under the curve for each of the bands using Image J.²

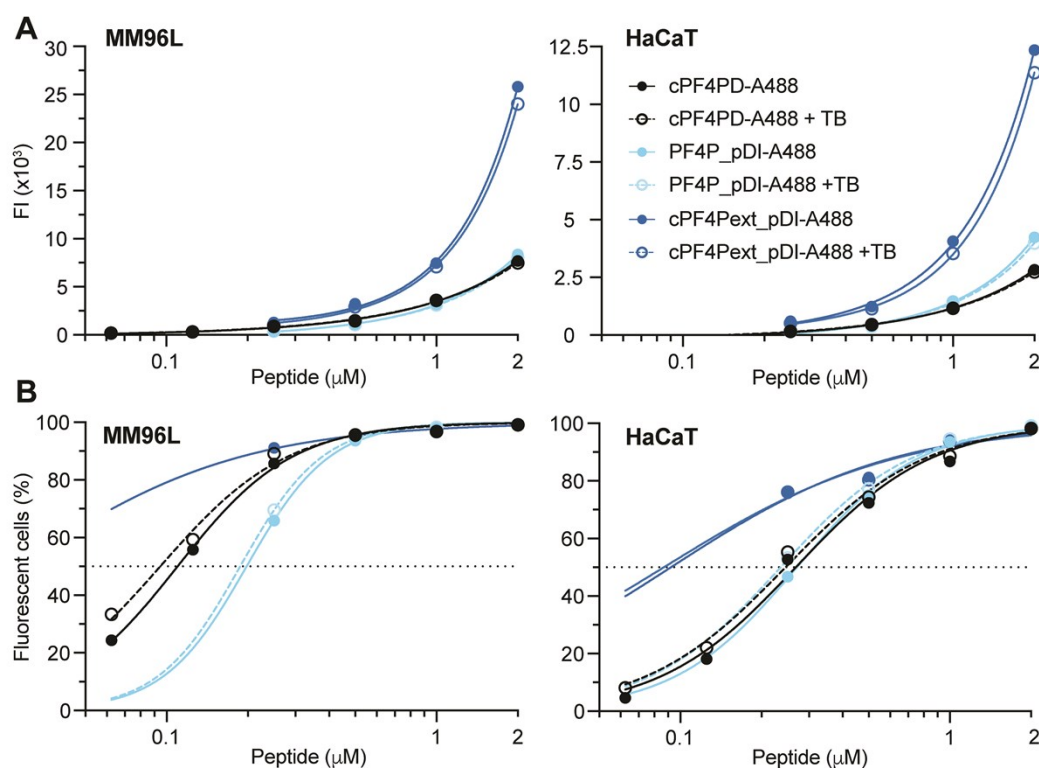


Figure S7. Internalization of A488-labeled peptides into the cytoplasm of MM96L and HaCaT cells without damaging the cell membrane. Cells were treated with 0.06–2 μM labeled peptide. Fluorescence emission intensity (FI) was recorded for 10000 cells using a 530/30 filter, and voltage setting of 370V for MM96L and 330V for HaCaT cells. Background FI for untreated cells was subtracted. FI was recorded again after addition of the fluorescence quenching molecule Trypan Blue (TB) to the same cell samples. Dose response curves show identical levels of internalized fluorescent peptide (A) and percentage of fluorescent cells (B) with and without treatment with TB. Identical FI in the presence or absence of TB indicates that the labeled peptide has an intracellular location, and that the cell membrane is intact. Data points are from a single representative experiment for each cell type. Curves were fitted using a least squares regression without weighting, using Prism (GraphPad software Inc), saturation binding with Hill slope ($\% \text{FC}_{50} = 100 \times [\text{peptide}]^H / (\text{FC}_{50}^H + [\text{peptide}]^H)$), where FC_{50} is the peptide concentration required to obtain 50% of fluorescent cells and H is the Hill slope).

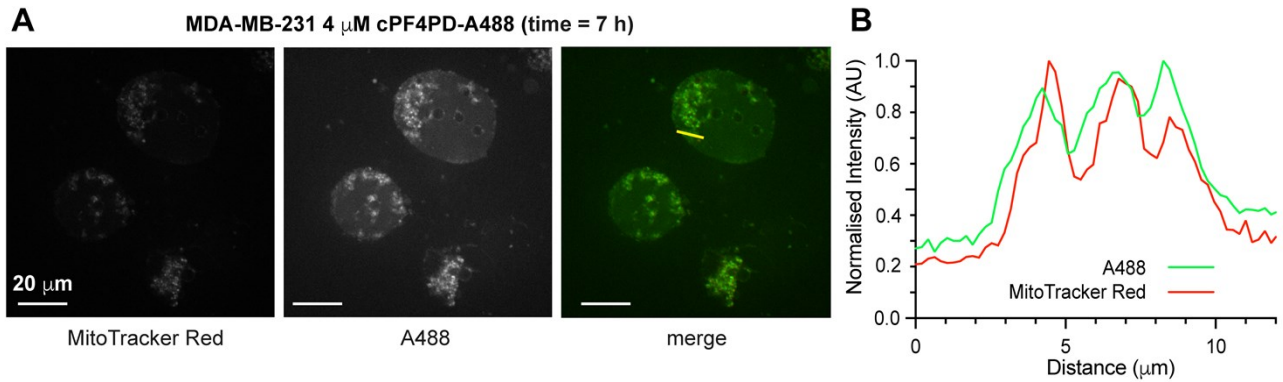


Figure S8. Colocalization of cPF4PD-A488 with mitochondrial membranes. (A) MDA-MB-231 cells were labeled with MitoTracker Red for 5 min and the dye was removed prior to treatment with 4 μ M cPF4PD-A488. Cells were monitored for seven hours. The seven hour time interval from **Figure 5C** is shown here for the MitoTracker Red channel (mitochondrial membranes), the A488 channel (labeled peptide) and the merged channels (colocalization of mitochondrial membranes and labeled peptide). The scale bars represent 20 μ m and a linear transect (12 μ m) is shown in yellow on the merged panel. (B) Fluorescence emission intensity of MitoTracker Red and A488 across the transect (A; right panel, yellow line) showing colocalization of the labeled peptide with mitochondrial membranes. The fluorescence signal was normalised to the maximum signal for each dye.

Movie S1. Internalization of 6 μ M PF4_pDI in MM96L cells. The outlined arrow indicates peptide located on the plasma membrane. After \sim 30 minutes, the peptide can be observed to localize in the cytoplasm (closed arrow head) and accumulate in mitochondria (double-headed arrow). Movie corresponds to **Figure 5B**.

REFERENCES

1. N. Lawrence, A. S. M. Dennis, A. M. Lehane, A. Ehmann, P. J. Harvey, A. H. Benfield, O. Cheneval, S. T. Henriques, D. J. Craik and B. J. McMorran, *Cell Chem. Biol.*, 2018, **25**, 1140-1150.
2. J. Schindelin, I. Arganda-Carreras, E. Frise, V. Kaynig, M. Longair, T. Pietzsch, S. Preibisch, C. Rueden, S. Saalfeld, B. Schmid, J.-Y. Tinevez, D. J. White, V. Hartenstein, K. Eliceiri, P. Tomancak and A. Cardona, *Nature Methods*, 2012, **9**, 676-682.